Energy Spectrum and Flux of Buoyancy-Driven Turbulence

Mahendra K. Verma*, Abhishek Kumar+ and Anando G. Chatterjee++

Department of Physics, Indian Institute of Technology Kanpur, Kanpur, 208016, India

*E-mail: *mkv@iitk.ac.in, +abhkr@iitk.ac.in and ++anandogc@iitk.ac.in*

Using direct numerical simulation we demonstrate that for isotropic stably-stratified flows follow Bolgiano-Obukhov scaling, i.e, the kinetic energy spectrum $E_u(k) \sim k^{-11/5}$, the entropy spectrum $E_\theta(k) \sim k^{-7/5}$, and kinetic energy flux $\Pi_u(k) \sim k^{-1/5}$. This is due to the conversion of kinetic energy to potential energy because of buoyancy. For Rayleigh Bénard convection, we argue that $\Pi_u(k)$ is a nondecreasing function of k due to the positive energy supply rate by buoyancy. Our numerical simulations show that the convection turbulence follows Kolmogorov-like scaling ($E_u(k) \sim k^{-5/3}$) with Kolmogorov's constant approximately 1.4.

Keywords: Startified turbulence; Rayleigh Bénard convection; Direct numerical simulation; Buoyancy-driven turbulence.

1. Introduction

Buoyancy-driven flows are observed in planets, stars, galaxies, as well as in electronic devices and industrial applications. Understanding of such systems are critical for modeling complex fluid flows, e.g., terrestrial atmosphere, weather predictions, planetary boundary layers, etc. One of the most important topic in this field is to study the scaling of spectrum and fluxes of kinetic energy (KE, $u^2/2$), and that of entropy ($\theta^2/2$). Here $\mathbf{u}$ and θ are the velocity and temperature fluctuations[1,2]. In this paper, we will compute these quantities using direct numerical simulations and show that the spectrum differs from Kolmogorov's theory when buoyancy is strong.

The dynamical equations describing the buoyancy-driven flows under the Boussinesq approximation are

$$\frac{\partial \mathbf{u}}{\partial t} + (\mathbf{u}\cdot\nabla)\mathbf{u} = -\frac{\nabla\sigma}{\rho_0} + \alpha g\theta\hat{z} + \nu\nabla^2\mathbf{u} + \mathbf{f^u}, \tag{1}$$

$$\frac{\partial \theta}{\partial t} + (\mathbf{u}\cdot\nabla)\theta = \frac{d\bar{T}}{dz}u_z + \kappa\nabla^2\theta, \tag{2}$$

$$\nabla\cdot\mathbf{u} = 0, \tag{3}$$

where $\mathbf{u}$ is the velocity field, θ and σ are the temperature and pressure fluctuations, respectively, with reference to the conduction state, $\hat{z}$ is the buoyancy direction, $\mathbf{f^u}$ is the external force field, d is the characteristic length, and ρ_0, ν, and κ are the fluid's mean density, kinematic viscosity, and thermal diffusivity respectively. Gravity-driven flows exhibit variety of nonlinear phenomena depending on the strength of gravity and the external forcing. We categorise these phenomena in terms of the important parameters of buoyancy-driven turbulence:

$$\text{Brunt Väisälä frequency } N_f = \sqrt{\frac{g}{\rho_0}\left|\frac{d\bar{\rho}}{dz}\right|} = \sqrt{\alpha g\left|\frac{d\bar{T}}{dz}\right|} \tag{4}$$

$$\text{Rayleigh number Ra} = \frac{d^4\alpha g}{\nu\kappa}\left|\frac{d\bar{T}}{dz}\right| \tag{5}$$

$$\text{Froude number Fr} = \frac{u_{\rm rms}}{dN_f} \tag{6}$$

$$\text{Richardson number Ri} = \frac{\alpha g d^2}{u_{\rm rms}^2}\left|\frac{d\bar{T}}{dz}\right| = \frac{1}{\text{Fr}^2} \tag{7}$$

$$\text{Reynolds number Re} = \frac{u_{\rm rms}d}{\nu} \tag{8}$$

$$\text{Prandtl number Pr} = \frac{\nu}{\kappa} \tag{9}$$

where $u_{\rm rms}$ is the rms velocity of flow. The Brunt Väisälä frequency is the frequency of the gravity wave, the Froude number is the ratio of the characteristic fluid velocity and the gravitational wave velocity, and the Richardson number is the ratio of the buoyancy and the nonlinearity $(\mathbf{u}\cdot\nabla)\mathbf{u}$.

The generic behaviour for various range of parameters are:

(1) **Stably stratified flows**: When $d\bar{T}/dz > 0$, the flow is stable and we observe the following behaviour.

  (a) *Internal gravity waves*: When the nonlinearity is weak (Re $\ll$ 1), we obtain internal gravity waves as the solution of the above equations. The frequency of gravity wave is N_f. Weak nonlinearity induces weak turbulence in the gravity waves.

  (b) *Quasi two-dimensional turbulence*: When the nonlinearity becomes significant and gravity too is strong (Fr $\ll$ 1), the flow along the buoyancy direction is suppressed, and it becomes quasi two-dimensional. Such flows have been studied extensively by Lindborg[3,4], Brethouwer *et al.*[5], and others.

(c) *Approximately isotropic turbulence*: When the gravity is relatively small but nonlinearity is strong (Re $\gg 1$), the flow becomes isotropically turbulent. When the Richardson number, which is the ratio of the buoyancy force and the nonlinearity, is of the order of unity, we obtain Bolgiano-Obukhov scaling (to be described below). However when the Richardson number is small, we obtain the usual Kolmogorov's spectrum.

(2) **Convective flows**: When $d\bar{T}/dz < 0$, the flow is intrinsically unstable and it becomes convective. The system exhibits convective rolls and patterns for small nonlinearity, but turbulence for large nonlinearity. We will show below that such flows in the turbulent limit exhibit approximate Kolmogorov's spectrum.

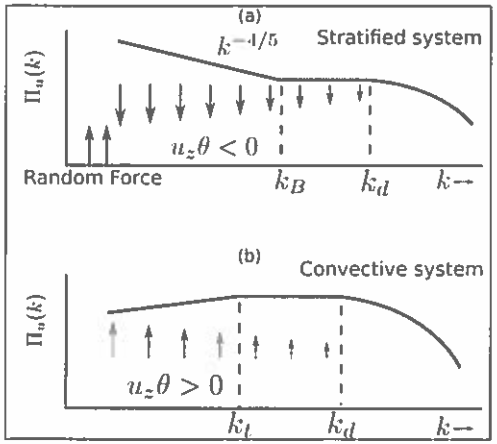

Fig. 1. Schematic diagrams of energy flux $\Pi_u(k)$: (a) In a stably stratified flow, $\Pi_u(k)$ decreases with k due to a negative energy supply rate $\Re\langle u_z(k)\theta^*(k)\rangle$. (b) In a thermally driven flow (e.g., Rayleigh Bénard convection), $\Pi_u(k)$ is a non-decreasing function of k (in inertial range) due to a positive $\Re\langle u_z(k)\theta^*(k)\rangle$. Thus $\Pi_u(k)$ first increases for $k < k_t$, where $F(k) > D(k)$, then $\Pi_u(k) = const$ $k_t < k < k_d$, where $F(k) \approx D(k)$; $\Pi_u(k)$ decreases for $k > k_d$ where $F(k) < D(k)$. Here k_d is the Kolmogorov's dissipation wavenumber. [Figure adapted from Kumar *et al.*[13]]

For stably stratified flows, Bolgiano[6] and Obukhov[7] first proposed a phenomenology, according to which

$$E_u(k) = c_1(\alpha^2 g^2 \epsilon_\theta)^{2/5} k^{-11/5}, \tag{10}$$

$$E_\theta(k) = c_2(\alpha g)^{-2/5} \epsilon_\theta^{4/5} k^{-7/5}, \tag{11}$$

$$\Pi_\theta(k) = \epsilon_\theta = \text{constant}, \tag{12}$$

$$\Pi_u(k) = c_3(\alpha^2 g^2 \epsilon_\theta)^{3/5} k^{-4/5}, \tag{13}$$

where k is the wavenumber, ϵ_θ is the entropy dissipation rate, $E_u(k)$ is the kinetic energy spectrum, $E_\theta(k)$ is the entropy spectrum, $\Pi_u(k)$ is the kinetic energy flux, and $\Pi_\theta(k)$ is the entropy flux, and c_i's are constants. The KE flux of a stably stratified flow is depleted at different length scales due to conversion of kinetic energy to "potential energy"; here $F(k) = \Re\langle u_z(k)\theta^*(k)\rangle < 0$. As a result, $\Pi_u(k)$ decreases with wavenumber (see Fig. 1(a)), and the energy spectrum is steeper than that predicted by Kolmogorov theory ($E(k) \sim k^{-5/3}$). The aforementioned scaling (Eqs. (1-4)) is referred to as *BO* scaling, while the usual Kolmogorov-scaling $k^{-5/3}$ is called Kolmogorov-Obukhov (*KO*) scaling. Note that the aforementioned scaling assumes that the turbulence is fully developed and isotropic. In this paper, we demonstrate that the stably stratified flows exhibit *BO* scaling when buoyancy is strong, and it exhibits *KO* scaling when the buoyancy is weak.

Procaccia and Zeitak[8], L'vov[9], L'vov and Falkovich[10], and Rubinstein[11] proposed that a similar scaling is also applicable to Rayleigh-Bénard convection (RBC) with the assumption that $F(k) < 0$. In this paper, we demonstrate using numerical simulations and phenomenological arguments that $F(k) > 0$ for RBC (see Fig. 1(b)). Consequently $\Pi_u(k)$ would increase with k, and $E_u(k)$ would be either Kolmogorov-like or shallower then $k^{-5/3}$. These observations of non-decreasing $\Pi_u(k)$ contradict the earlier predictions on RBC[8-10], but they are in agreement with the numerical results of Škandera *et al.*[12]. For further details see Kumar *et al.*[13] and Verma *et al.*[14].

2. Numerical Methods

We solve the following non-dimensionalized form of Eqs. (1,2,3):

$$\frac{\partial \mathbf{u}}{\partial t} + (\mathbf{u}\cdot\nabla)\mathbf{u} = -\nabla\sigma + \theta\hat{z} + \sqrt{\frac{\mathrm{Pr}}{\mathrm{Ra}}}\nabla^2\mathbf{u} + \mathbf{f}^{\mathbf{u}}, \tag{14}$$

$$\frac{\partial \theta}{\partial t} + (\mathbf{u}\cdot\nabla)\theta = Su_z + \frac{1}{\sqrt{\mathrm{RaPr}}}\nabla^2\theta, \tag{15}$$

$$\nabla\cdot\mathbf{u} = 0. \tag{16}$$

These equations have been nondimensionalized using d as the length scale, $\sqrt{\alpha g \Delta d}$ as the velocity scale, and Δ as the temperature scale. The parameter $S = (d\bar{T}/dz)/(\Delta/d)$, where Δ is the absolute temperature differences

in height d, takes values ± 1. For RBC, the temperature of the top plate is lower than that of bottom one, hence $S = +1$, but for the stably stratified flows, the temperature gradient is opposite, i.e., $S = -1$.

We perform our direct numerical simulation of the above equations using a pseudospectral code Tarang[15] in a three-dimensional periodic box of size $(2\pi)^3$. We use fourth-order Runge-Kutta (RK4) method for time stepping, Courant-Freidricks-Lewey (CFL) condition for computing time step Δt, and 3/2 rule for dealiasing. We apply a random force to the flow in the band $2 \le k \le 4$ using the scheme of Kimura and Herring[16] to obtain a steady turbulent flow.

For RBC, we performed a simulation in unit box with 512^3 grid. For the horizontal plates, we employ a free-slip boundary condition for the velocity field and a conducting boundary condition for the temperature field. For the vertical walls, we apply a periodic boundary condition for both fields. Note that for RBC $\mathbf{f^u} = 0$ since the buoyancy makes the flow turbulent by itself.

3. Results and Discussions

3.1. *Stably stratified turbulence*

Table 1. Parameters of our numerical simulations for stably stratified turbulence (SST) and Rayleigh Bénard convection (RBC): flow type, grid size, Rayleigh number Ra, Richardson number Ri, Froude number Fr, Reynolds number Re, kinetic energy dissipation rate ϵ_u, thermal dissipation rate ϵ_θ, and averaged Δt. We choose Prandtl number Pr = 1 for both the runs.

Flow Type	Grid	Ra	Ri	Fr	Re	ϵ_u	ϵ_θ	Δt
SST	1024^3	5×10^3	0.01	1.4	649	114	150	3.5×10^{-6}
RBC	512^3	10^7	16	NA	790	8.8×10^{-3}	10^{-3}	6.2×10^{-4}

We perform large-resolution simulations for Pr = 1 and Rayleigh number $\mathrm{Ra} = 5 \times 10^3$. We report our results when the flow has reached a steady state. We find that the Richardson number Ri = 0.01. Thus buoyancy is comparable to the nonlinear term in our simulation. The other parameters of our runs are listed in Table 1.

We compute the KE and entropy spectra and fluxes for the steady-state data of the above run. Figures 2(a, b) indicate that the *BO* scaling fits with the numerical data better than the *KO* scaling. The KE and entropy

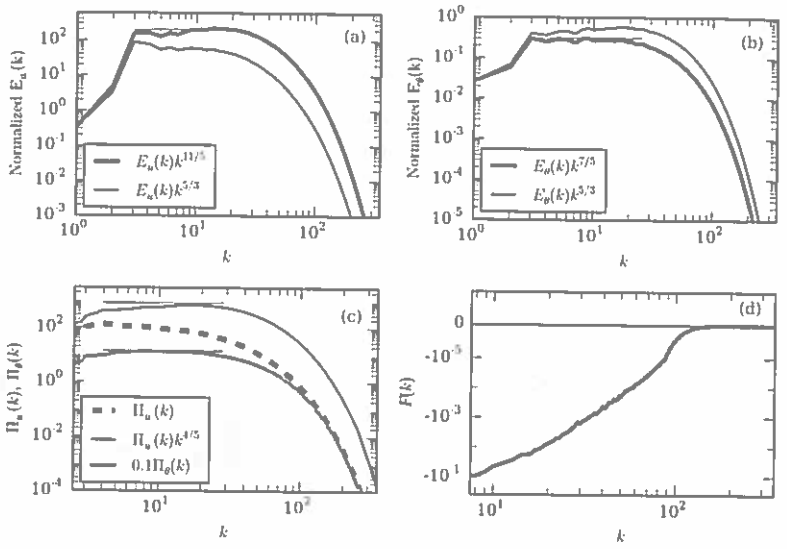

Fig. 2. For stably stratified turbulence (SST) with Pr = 1 and Ri = 0.01, plots of (a) normalized KE spectra, (b) normalized entropy spectra for Bolgiano-Obukhov (*BO*) and Kolmogorov-Obukhov (*KO*) scaling, (c) KE flux $\Pi_u(k)$, normalized KE flux $\Pi_u(k)k^{4/5}$, and entropy flux $\Pi_\theta(k)$, and (d) negative $F(k)$ for stably stratified flow.

fluxes are plotted in Fig. 2(c). Clearly, the KE flux $\Pi_u(k)$ is positive, and it decreases approximately as $k^{-4/5}$, consistent with the *BO* predictions [Eq. (13)]. The entropy flux Π_θ is a constant, and the energy supply rate by buoyancy, $F(k) = \Re\langle u_z(k)\theta^*(k)\rangle$, is negative (see Fig. 2(d)). These results show that the *BO* scaling is valid for stably stratified flows for Ri = O(1). We remark that the flow is approximately isotropic.

3.2. *Rayleigh Bénard convection with* Pr = 1

We performed a numerical simulation of RBC with for Pr = 1 and Rayleigh number $\mathrm{Ra} = 10^7$ (see Table 1). We employ free-slip boundary condition for our simulation. We report the spectra and fluxes of kinetic energy and entropy $(\theta^2/2)$ after the flow has reached a steady state.

In Fig. 3(a), we plot the normalized KE spectra for the *BO* and the *KO* scaling. The plots indicate that the *KO* scaling fits better than the *BO* scaling for a narrow band of wave numbers (the shaded region, $15 < k < 40$). In Fig. 3(b), we plot the entropy spectrum that exhibits a dual branch, with the upper branch scaling as k^{-2}, whose origin is related to the

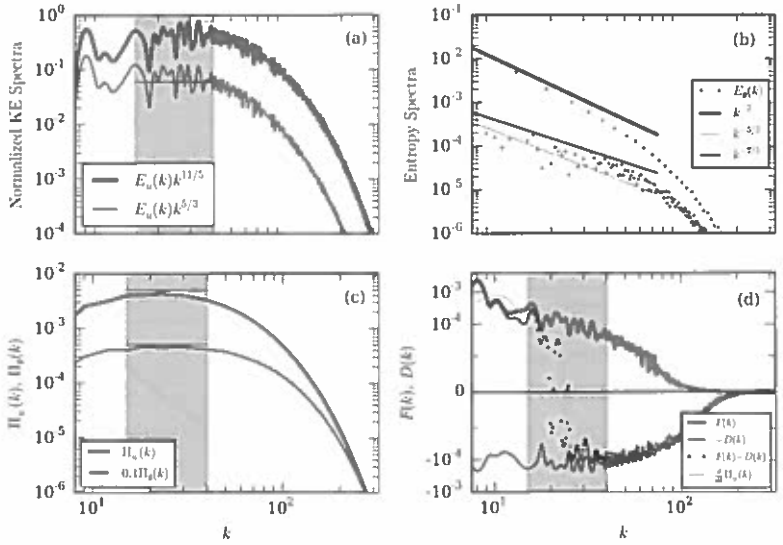

Fig. 3. For convective turbulence (RBC) with Pr = 1 and Ra = 10^7, plots of (a) normalized KE spectra for (BO) and (KO) scaling; (b) entropy spectrum that exhibits a dual branch. The upper branch of $E_\theta(k)$ matches with k^{-2} quite well, while the lower part is fluctuating. (c) KE flux $\Pi_u(k)$ and entropy flux $\Pi_\theta(k)$; (d) $F(k)$, $D(k)$, $F(k) - D(k)$, and $d\Pi_u(k)/dk$. Shadow region shows the inertial range.

observation that $\hat{\theta}(0, 0, 2n) \approx -1/(2n\pi)$, where $\hat{\theta}$ is the Fourier transform of the temperature fluctuations[17]. The KE and entropy fluxes, shown in Fig. 3(c), demonstrate that the fluxes are constant, consistent with the KO scaling.

For RBC we observe that $F(k) > 0$, as shown in Fig. 3(d). In Fig. 3(d), we also plot $D(k)$, $F(k) - D(k)$, and $d\Pi_u(k)/dk$. For the wavenumbers band $15 < k < 40$, $F(k) \approx D(k)$, hence $d\Pi_u(k)/dk \approx 0$ or $\Pi_u(k) \approx const.$ This constant KE flux yields $E_u(k) \sim k^{-5/3}$. Note that the aforementioned Kolmogorov's $-5/3$ spectrum is not due to a constant energy flux, but due to a cancellation of the energy supply rate with the dissipation rate. For our run, the Reynolds number Re ≈ 790, which is moderate. For Re ≈ 790, the Kolmogorov's length is $\eta = \mathrm{Re}^{-3/4}L \approx L/133$, where $L = 1$ is the size of the box. Consequently the dissipation starts at the length $l_d = 60\eta \approx L/2$ or at the wavenumber of $k_d = 2\pi/l_d \approx 4\pi$, which is consistent with our results exhibited in Fig. 3.

The aforementioned arguments show that the behaviour of $F(k)$ and

$\Pi_u(k)$ for the stably stratified flow and RBC are quite different[13]. Our numerical results are consistent with our flux-based arguments, but they differs from those of Procaccia and Zeitak[8], L'vov[9], and L'vov and Falkovich[10].

We also compute Kolmogorov's constant for the above run. We find that in the inertial range $\Pi_u \approx \epsilon_u \approx 8.8 \times 10^{-3}$, and $E_u(k)k^{5/3} \approx 0.06$. Therefore,

$$K_{Ko} = \frac{E_u(k)k^{5/3}}{\Pi_u^{2/3}} \approx 1.4, \tag{17}$$

which is in agreement with the theoretical and experimental estimates.

The Richardson number for the RBC run is approximately 16, which is related to the Péclet number Pe as following:

$$\begin{aligned} \mathrm{Ri} &= \frac{\alpha g d(d\bar{T}/dz)}{u^2/d} \\ &= \frac{\alpha g d^4(d\bar{T}/dz)}{\nu\kappa}\frac{\nu}{\kappa}\frac{\kappa^2}{u^2 d^2} \\ &= \frac{\mathrm{RaPr}}{\mathrm{Pe}^2}. \end{aligned} \tag{18}$$

Verma *et al.*[18] showed that

$$\mathrm{Pe} \approx 0.24\sqrt{\mathrm{RaPr}}. \tag{19}$$

Hence Ri $\approx 1/0.24^2 \approx 16$, which matches very well with our numerical results.

3.3. *Rayleigh Bénard convection for small and large* Pr

For RBC, the turbulence behaviour for very small or very large Prandtl number differs significantly from that with moderate Prandtl numbers (Pr ~ 1). For zero and small Prandtl number, Mishra and Verma[17] showed that the temperature fluctuations and hence the buoyancy are concentrated at low wavenumbers. This feature makes Kolmogorov phenomenology applicable for zero and small Prandtl numbers. Therefore the kinetic energy spectra for zero and small Prandtl number are Kolmogorov-like.

For infinite and large Prandtl numbers, Pandey *et al.*[19] showed that the viscous dissipation dominate the nonlinear term $\mathbf{u} \cdot \nabla \mathbf{u}$. Consequently, the kinetic energy spectrum scales $k^{-13/3}$. The entropy spectrum exhibits dual branch (k^{-2} and another branch) for all Prandtl number flows.

In summary, RBC turbulence with small to moderate Prandtl numbers exhibit Kolmogorov scaling, while that with large and infinite Prandtl number exhibit $E_u(k) \sim k^{-13/3}$.

4. Summary and Conclusions

In summary, we analyse stably-stratified and convective turbulence using numerical simulations. For the stably-stratified flows, we restrict ourselves to approximate isotropic regime that occurs for Fr $\gtrsim 1$ and Ri $\lesssim 1$. For such stably stratified flows, our numerical results on the energy spectrum, the energy flux, and the energy supply rate by buoyancy reveal that they exhibit Bolgiano-Obukhov *BO* scaling. We show that the energy supply rate due to buoyancy, $F(k)$, is negative, hence the kinetic energy is transferred to the potential energy, which is dissipated.

We remark that the stably stratified flows become quasi two-dimensional when Fr $\ll 1$. The turbulent behaviour of such flows is very different, and it is being actively studied[3,4].

For turbulence in RBC with moderate Prandtl number, we show that the kinetic energy flux is a non-decreasing function of k (since $F(k) > 0$), and the energy spectrum of KE cannot be steeper than $k^{-5/3}$ in the bulk. We observe $k^{-5/3}$ energy spectrum for kinetic energy. The flux of kinetic energy and entropy remain approximately constant here. We estimate Kolmogorov's constant to be around 1.4, which is in a very good agreement with theoretical and numerical results. When combined with earlier work on RBC, convective turbulence with small to moderate Prandt numbers exhibit Kolmogorov scaling, while that with large and infinite Prandtl number exhibit $E_u(k) \sim k^{-13/3}$.

5. Acknowledgments

We thank K. R. Sreenivasan, Anindya Chatterjee, Pankaj Mishra, and Mani Chandra for useful comments and suggestions, and T. K. Sengupta and the organizers for hosting the wonderful and interactive IUTAM meeting. We also thanks the editors of the proceedings for the useful suggestions on the paper. Our numerical simulations were performed at Centre for Development of Advanced Computing (CDAC) and IBM Blue Gene P "Shaheen" at KAUST supercomputing laboratory, Saudi Arabia. This work was supported by a research grant SERB/F/3279/2013-14 from Science and Engineering Research Board, India.

References

1. E. D. Siggia, *Ann. Rev. Fluid Mech.* **26**, 137 (1994).
2. D. Lohse and K. Q. Xia, *Ann. Rev. Fluid Mech.* **42**, 335 (2010).
3. E. Lindborg, *Geo. Res. Lett.* **32**, L01809 (2005).
4. E. Lindborg, *J. Fluid Mech.* **550**, 207 (2006).
5. G. Brethouwer, P. Billlant, E. Lindborg, and J.-M. Chomaz *J. Fluid Mech.* **585**, 343 (2007).
6. R. Bolgiano, *J. Geophys. Res.* **64**, 2226 (1959).
7. A. N. Obukhov, *Dokl. Akad. Nauk SSSR* **125**, 1246 (1959).
8. I. Procaccia and R. Zeitak, *Phys. Rev. Lett.* **62**, 2128 (1989).
9. V. S. L'vov, *Phys. Rev. Lett.* **67**, 687 (1991).
10. V. S. L'vov and G. E. Falkovich, *Physica D* **57**, 85 (1992).
11. R. Rubinstein, Icqmp-94-8, cmott-94-2, *NASA Tech. Memo.* (1994).
12. D. Škandera, A. Busse, and W. C. Müller, *High Performance Computing in Science and Engineering, (Springer, Berlin), Part IV*, 387 (2008).
13. A. Kumar, A. G. Chatterjee and M. K. Verma, *Phys. Rev. E* **90**, 023016 (2014).
14. M. K. Verma, A. Kumar, and A. G. Chatterjee, *Physics Focus* **25(1)**, 45 (2015).
15. M. K. Verma, A. G. Chatterjee, K. S. Reddy, R. K. Yadav, S. Paul, M. Chandra, and R. Samtaney, *Pramana* **81**, 617 (2013).
16. Y. Kimura and J. R. Herring, *J. Fluid Mech.* **698**, 19 (2012).
17. P. K. Mishra and M. K. Verma, *Phys. Rev. E* **81**, 056316 (2010).
18. M. K. Verma, P. K. Mishra, A. Pandey, and S. Paul *Phys. Rev. E* **85**, 016310 (2012).
19. A. Pandey, M. K. Verma, and P. K. Mishra *Phys. Rev. E* **89**, 023006 (2014).